Mechatronics and Making Mid-Term Project Report Exoskeleton Robotic Hand with Wolf Claw Mechanism

Bryan Li – SN 25003743
Yan Pei Zhu – SN 25103352
Nolan Yu – SN 25113715

October 31, 2025

Contents

1 Project Objectives and Description

We examined the percentage of people who were victims of stalking in the last year, with 19.9% of women since the age of 16 suffering from this abuse, of which 8.05% (of total victims) were single women[2]. This data highlights the significance of our mechanism, as it enhances safety of the victim when physically approached by the stalker. However, this mechanism would be considered a weapon with the intention of using it for self-defence, which violates the Criminal Justice and Immigration Act 2008[5]. Thus, to legalise our mechanism, we modified the dangerous component (the three wolf claws) into a blunt claw-shaped design made of PLA materials. With the aim of this mechanism serving as a cosplay prop and the objective of helping with self-defence, this aspect will be further examined in section 2.3, wolf claw mechanism comparison.

1.1 Similar Mechanisms

There are many applications of exoskeleton robotic hands in diverse fields (e.g. rehabilitation medicine) in which most of these exoskeleton hands are powered. Powered exoskeleton robotic hands tend to have higher demands regarding control schemes and mechanical design (involving actuators) whereas our mechanism allows a lightweight approach and only relies on the user's instinctive movements.

The robotic hand should have the same DOFs as a human, yet given the compact size of the hand, it becomes impractical to actively control every joint[3] when the complexity of the control algorithms increases with the DOFs in a powered exoskeleton robotic hand. Thus, some motions are left passive (passive DOF), power and control signals of the hand must also be routed such that it does not interfere with motion of arm, where we will be placing the wolf claw mechanism. Taking the increased mass and inertia into consideration, we have decided to design our mechanism in a purely mechanical (passive) way since there is no reliance on power source and is less susceptible to technical malfunctions.

A 1 DOF kinematic architecture[4] has been used for the DIP (distal Interphalangeal joint) and PIP (Proximal Interphalangeal joint) as it enables a precise replication of the natural grasping motion.

1.2 Industrial Applications

The exoskeleton robotic hand of our mechanism is purely passive, providing support for the fingers and hand during tasks that require a sustained grip on tools for long periods. By redistributing the physical load from the fingers to the palm exoskeleton (connected to the wrist and arm) and supporting proper posture, the user is less likely to suffer from overuse injuries. This mechanism could be used for repetitive tasks, such as manual labour in construction, and it is applicable in further designing or developing powered exoskeleton hands.

2 Mechanical and Mechanism Analysis

2.1 Drive Method and Transmission

This robotic hand exoskeleton uses an acceleration-based machinery system, amplifying the movements of the finger.

This is achieved using a planetary gear mechanism connected to a string transmission and a pulley and belt system.

Details of the transmission process shown below:

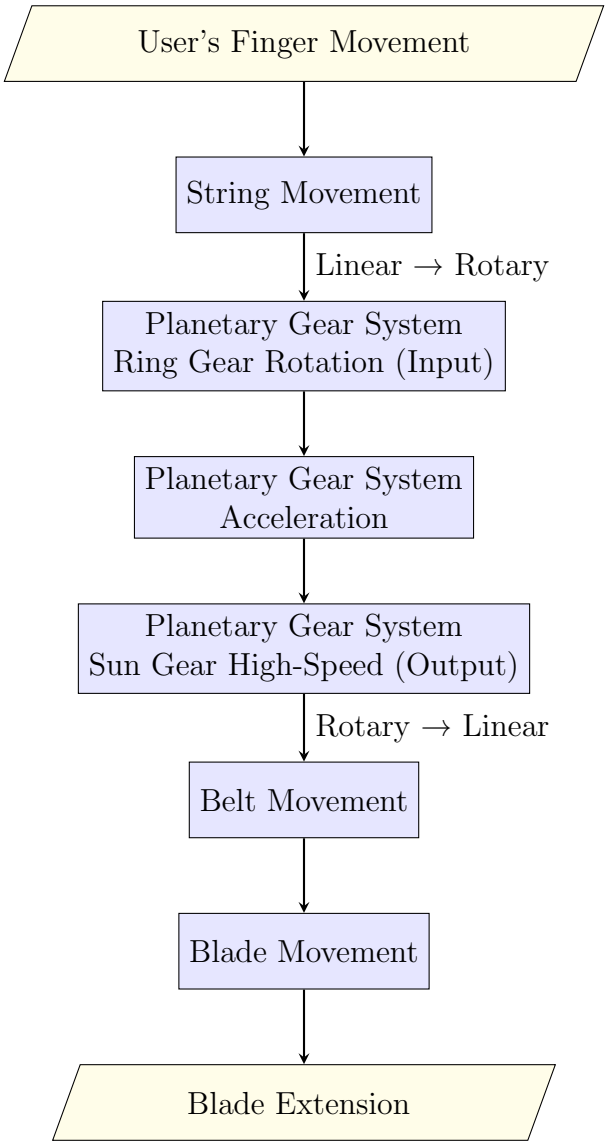

2.2 Hand Exoskeleton Mechanisms Comparison

2.2.1 Hand Biomechanics

The exoskeleton design is based on the anatomy of a hand (Figure 1), consisting of 19 bones and 14 joints[2], excluding the carpal bones. The exclusion of the carpal bones (eight small bones in total) limits the extent the user's hand can bend whilst wearing this exoskeleton hand, this was deliberately chosen based on multiple factors such as the increasing mass and inertia of the exoskeleton, the noise generated from the movement of fingers and the limited space to securely link the carpal bones whilst not affecting the overall movement of adjacent fingers.

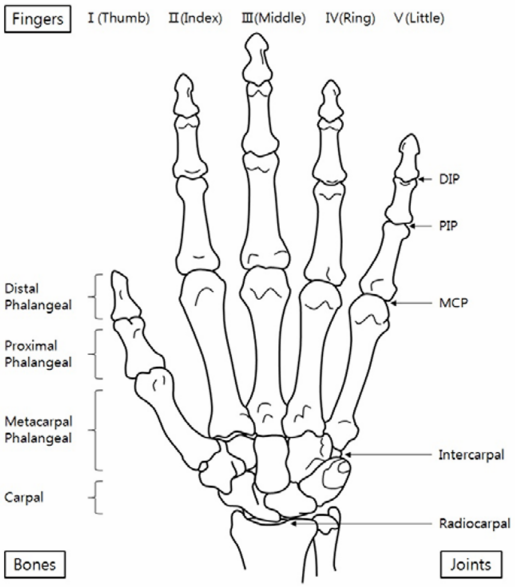

(a) bones and joints of a human hand[1]

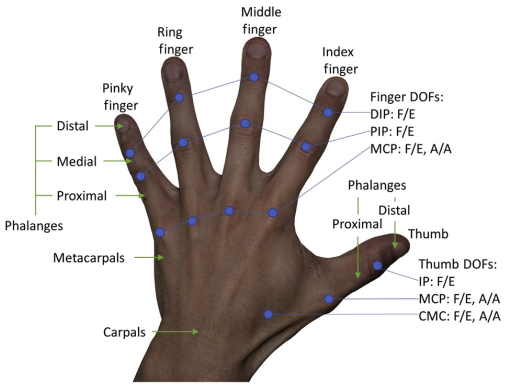

(b) model of human hand[3]

Figure 1: Human Hand

DOF of finger joints[3]

Metacarpophalangeal joint (**MCP**):
2 DOF (flexion/extension, abduction/adduction)

Distal Interphalangeal joint (**DIP**) and Proximal Interphalangeal joint (**PIP**):
1 DOF (flexion/extension), this is a 1 DOF kinematic architecture

Carpometacarpal joint (**CMC**):
2 DOF (flexion/extension, abduction/adduction), a saddle joint, allowing circumduction and opposition movements. There is a third degree of freedom in the thumb that enables axial rotation/opposition which we have not included as it is unnecessary for the aim and objective of our mechanism, increasing the mechanical complexity, mass and inertia.

The resting position for these joints is slight flexion, the exoskeleton hand must also be at this position when at rest to increase joint laxity and to prevent joint stiffness and contractures, which is ideal for immobilisation and rehabilitation. In the resting

position[1], the MCP joint is in 35 deg – 45 deg of flexion, PIP joint: 30 deg – 45 deg, DIP joint: 10 deg – 20 deg.

Wrist Structure Analysis

The human wrist has 3 degrees of freedom: flexion/extension, radial/ulnar deviation and pronation/supination. Reflecting upon the objective of our design, we consciously excluded the pronation/supination rotational axis, which is where the forearm is rotated to turn the palm since this would lead to the user being injured more easily.

2.2.2 Selection of Mechanism Type

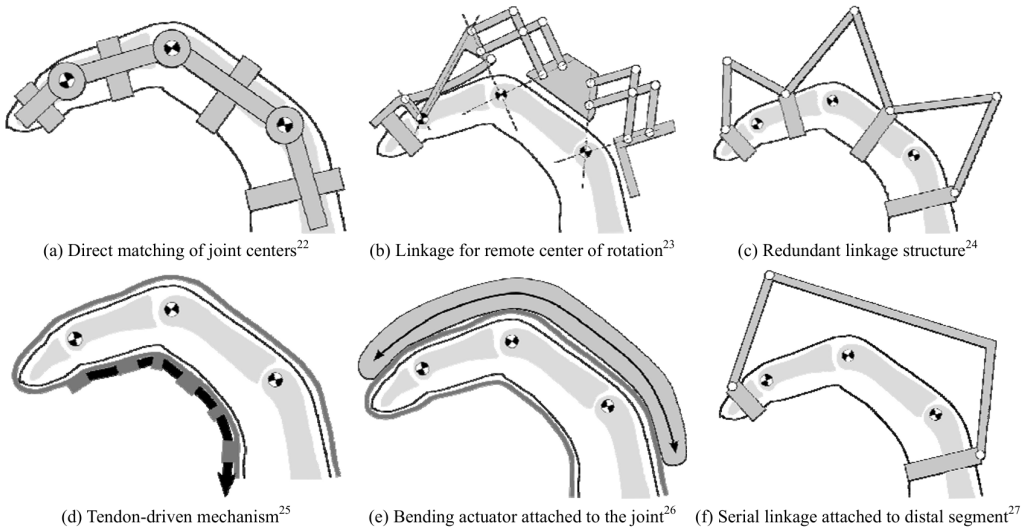

(a) Direct matching of joint centers[22] (b) Linkage for remote center of rotation[23] (c) Redundant linkage structure[24]

(d) Tendon-driven mechanism[25] (e) Bending actuator attached to the joint[26] (f) Serial linkage attached to distal segment[27]

Figure 2: mechanism types[1]

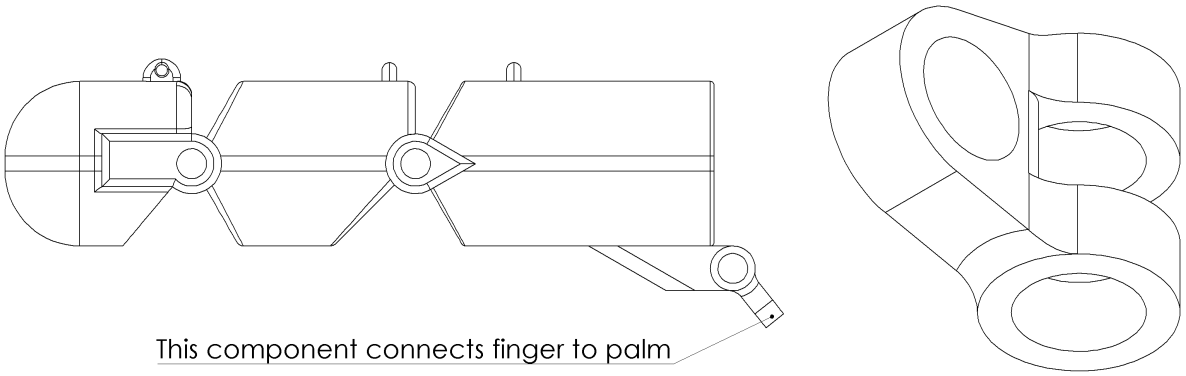

(a) configuration of how component connects fingers to palm (b) component allowing 2 DOFs in MCP join

Figure 3: finger with linkage component

The direct matching of joints (Figure 2a) provides a structurally simple and compact solution, removing unnecessary components including complex actuation and additional linkages. This arrangement minimises mechanical complexity and simplifies fabrication and control, taking inspiration from this design, we have adapted the structure to allow

2 DOFs for the MCP joint. This is achieved by connecting part of the MCP joint with another component using a rod, with an identical component being linked to the palm exoskeleton (see figure 3).

For the objective to be executed safely, a physical stopper would be placed on both sides of the wrist exoskeleton to prevent the hand from bending backwards. The fingers are also at risk of bending backwards, hence, increasing the thickness of the palm exoskeleton and creating indentations would decrease the strain on the fingers by distributing the force over the volume of the indentations.

To further reduce this strain, a layer of rubber (or any material with a high friction coefficient) could be added to the tip of the fingers and the indentations in the palm. Consequently, we must consider whether the user would be able to clench their firt quickly enough in a life-threatening situation.

2.3 Wolf Claw Mechanism

Design of wolf claw

Consider a wolf claw made of multiple sections:

For this prototype the whole mechanism would be more portable due to the retractable features. For these retractable features to be implemented, the inner structure of each section of the wolf claw would be hollow, with only the tip of the claw being solid.

The main challenges in this include how each section is going to connect as the number of sections increase, thus each section becomes thinner and the room for connection between adjacent links being reduced. When this wolf claw is extended, it becomes difficult to ensure the same section of each wolf claw extends simultaneously, smoothly and securely. As a consequence of not having any supports in the wolf claw, there will be oscillations in each section, with the tip of the wolf claw oscillating the most. Reflecting on the objective of this mechanism, this prototype is ineffectual as the structure of this wolf claw would lead to the sections easily snapping.

Therefore, we propose a different method, where each wolf claw is modelled as individual blades since it would remain consistent with the defined aim and objective. However, this approach would lead to the box containing the wolf claw mechanism being longer, problems that arise from this include how this housing is going to be stabilised to the arm as it would be longer than a forearm of the average human.

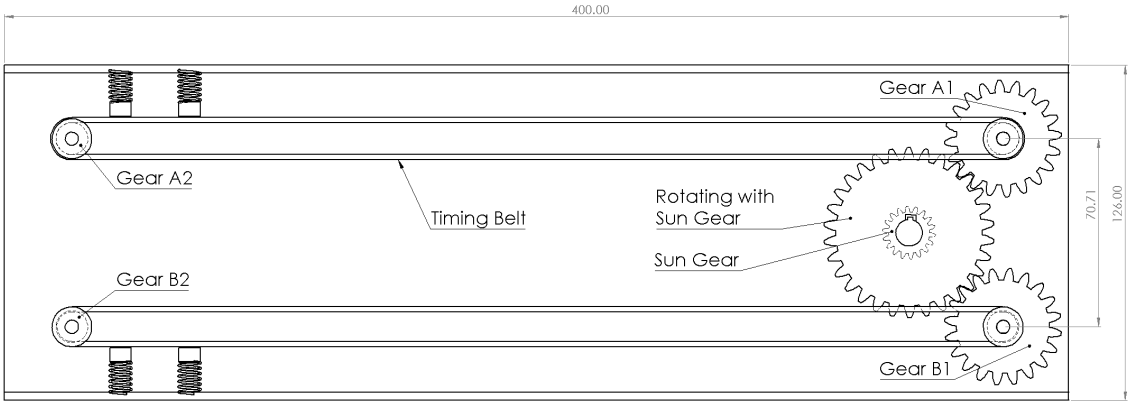

Figure 4: belt-pulley assembly with simple secondary gear train

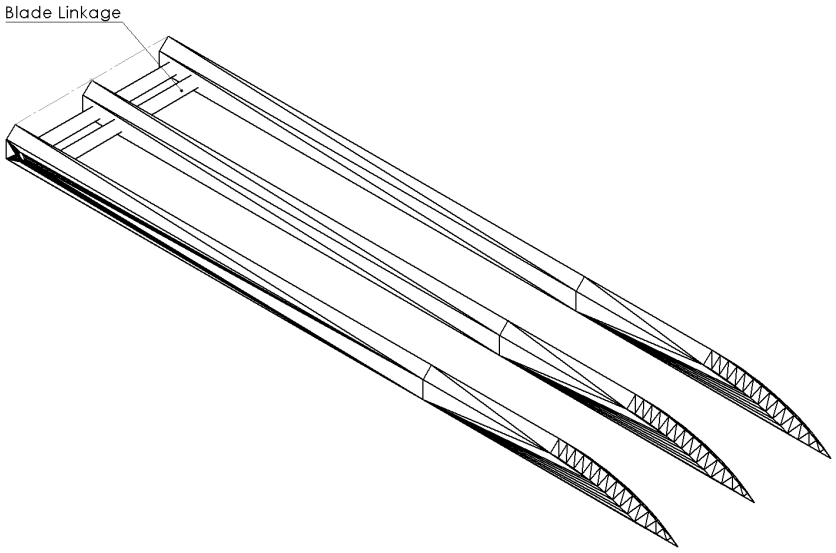

Figure 5: blade assembly

The three blades (Figure 5) are connected by drilling two holes near the end of the blade and inserting two rods to increase stability, perpendicular to the direction of the blades. These blades are not sharpened since the purpose is to act as a cosplay prop, but to fulfil the objective effectively, these blades would have a sandpaper coating and be non-backdrivable. To include this non-backdrivable feature, two spring plungers are integrated at the side of the box (two for redundancy), locking the two side blades in position. In this mechanism we aim to make to make the wolf claw retract semi-automatically, hence we modified the spring plungers (see Figure 4) so that they can retract by applying force to the handle of the spring plunger. By connecting a fixed section of the timing belt to the side of the box, the blades can retract semi automatically when the spring plungers are retracted.

Transmission Mechanism Selection

The key feature of our design is sliding the wolf claws out, this achieved using a combination of compound planetary gear as part of a simple secondary gear train. Another approach for this would be using the structure of a compound gear train, let the two

versions be versions one and two respectively. Both methods start with rotary-to-rotary motion, this is then converted from rotary to translational motion through the use of pulley and belt systems.

Version I: Planetary Gear

This version provides a higher gear ratio with a more compact and stable design but requires high precision in laser cutting and 3D printing as several components mesh into the same gear.

Version II: Compound Gear Train

This version is simpler to print and has a higher flexibility in gear ratios, yet there is a lack of stability in the blades as the centre blade drives the two side blades. When force is applied to the blades, this design is more susceptible to structural failure.

Therefore, we would use version 1 for our first prototype.

2.3.1 Version I: Planetary Gear

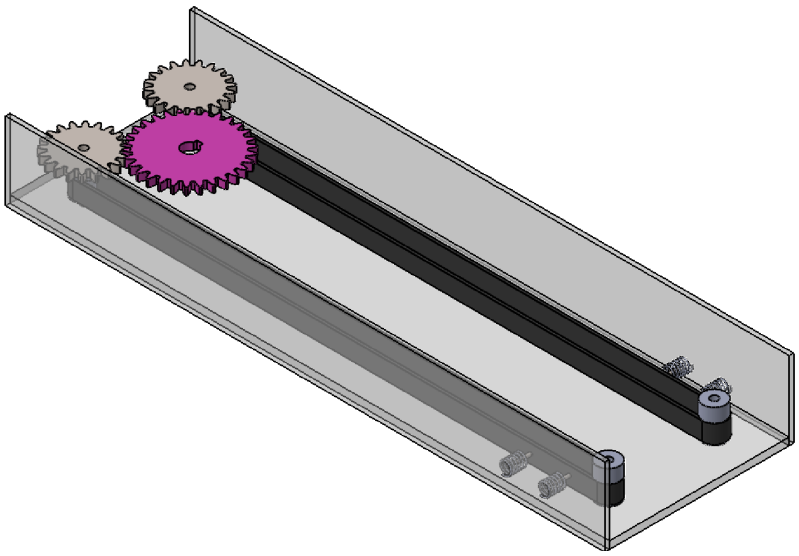

Figure 6: side view of version I

The light inextensible string would be connected to the ring gear of the fixed carrier planetary gear. The fixed carrier gear would be screwed to the top of the box, this enabling the planetary gear to hang from above. The sun gear is connected to another gear that would mesh with two identical gears, gears A_1 and B_1, fixed to the bottom of the housing by screws (Figure 6). This forms a simple secondary gear train, further increasing the overall gear ratio.

At the other end of the box, identical gears to A_1 and B_1 are fixed to the floor parallel to gears A_1 and B_1, let us call them A_2 and B_2. By using timing belts (shown in Figure 4), two pulleys and belts systems are formed between gears $A_{1,2}$ and $B_{1,2}$, increasing efficiency

with no slippage. Challenges in this design being the non-backdrivable timing belts being difficult to manufacture as the timing belts are required to be flexible for our design. When 3D printing each section of the timing belts, removing the supports was an arduous task with low success rates, hence we adapted the gears $A_{1,2}$ and $B_{1,2}$ as shown in figure 4 to use the open timing belts and timing pulleys in the innovation lab. The top section will enable the gears A_1 and B_1 to mesh properly with the sun gear, the bottom half would be glued into the timing pulley, meaning that gears A_2 and B_2 would just be a timing pulley with a fixed rod through the centre, fixed to the bottom of the housing.

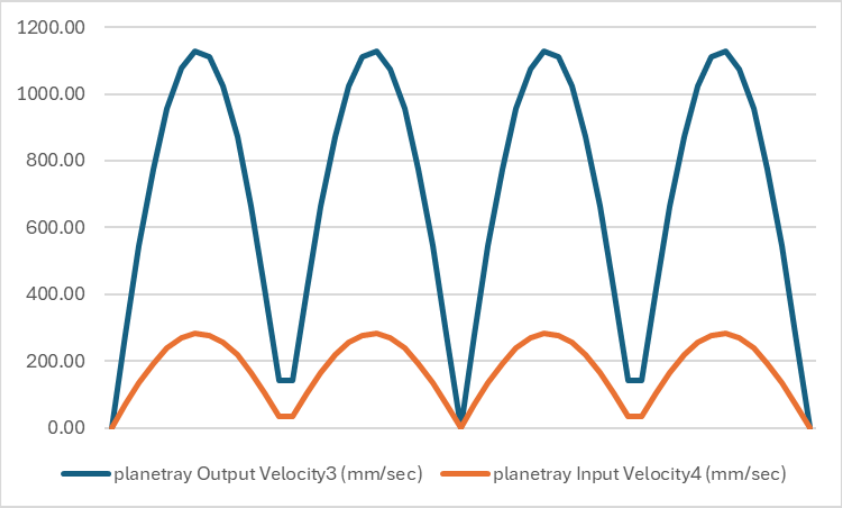

Figure 7: Linear velocity of input and blade out

The two side blades would be fixed to these pulley and belt systems (A_1,2 and $B_{1,2}$) using superglue on the end of the blade, with a centre blade connected to a third pulley and belt system. The blades are connected to ensure all three blades slide out simultaneously, and stability of the centre blade can be increased by integrating a third pulley and belt system. This allows the motion of the centre blade to be parallel to the side blades when the whole mechanism is moving or when there is a force applied to the tip of the blades. When there is force applied on the blades, it may be impractical to hold the blades to the belt only by superglue at the end section of the blade, hence screwing the blades to the belt would maintain the position of the blades. Ensuring the open timing belts are tight would be challenging as the glue requires some time to dry and the timing belts must be held together tightly during this time, the difficulty in this being that it must align perfectly with the other end to ensure completely horizontal motion of blades.

2.3.2 Version II: Compound Gear Train

The compound gear train (Figure 8a) is dependent on the contact between gears, reflecting on the objective of our mechanism, it is essential to ensure the gears mesh regardless of motion of mechanism.

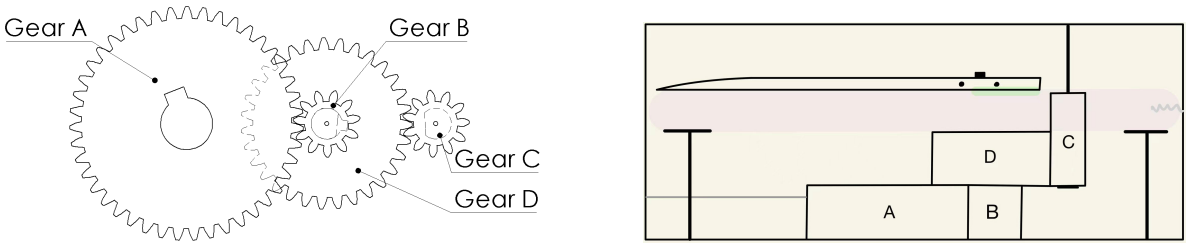

(a) compound gear train

(b) compound gears, pulley and belt system

Figure 8: design of version II

Gear A will be connected to the floor by a screw, similar to gears $A_{1,2}$ and $B_{1,2}$ in version one, this screw will ensure the gears are in a fixed position yet allow rotational movement to enable meshing between gears. The same procedure has been utilised for gears B and D, with gear C resting on an upside-down "T" shaped support which is fixed to the top of the housing. Gear C has been modified to a similar design to gears A_1 and B_1, with the upper half glued into the timing pulley and the lower half meshing with gear D.

The pulley and belt system of this version would be supported by two "T" shaped supports, with the end of the centre blade screwed to the side of the timing belt. In this version, the centre blade provides the driving force to the two side blades. To increase the stability of the blades, another two pulley and belt systems guides the motion of the side blades. The timing pulleys would be supported by a vertical rod with two horizontal plates, this support would be made of three components, these three components ensure that the supports are fully vertical. The difficulty of this involves glueing the supports vertically (in the box) and parallel to the other pulley and belt transmissions.

3 Mathematical Modelling and Analysis

3.1 Fingers and Wrist Modelling

Finger and Overhead String Movement

The light, inextensible string is tied to the loop on the DIP joint, and is guided through the other loops, with the other end connected to the ring gear of the planetary gear. The linear movement of the string is created by the finger's flexion, see figure 9.

Figure 9a describes the details and data when finger curved, Figure 9b describes the details and data when finger extended.

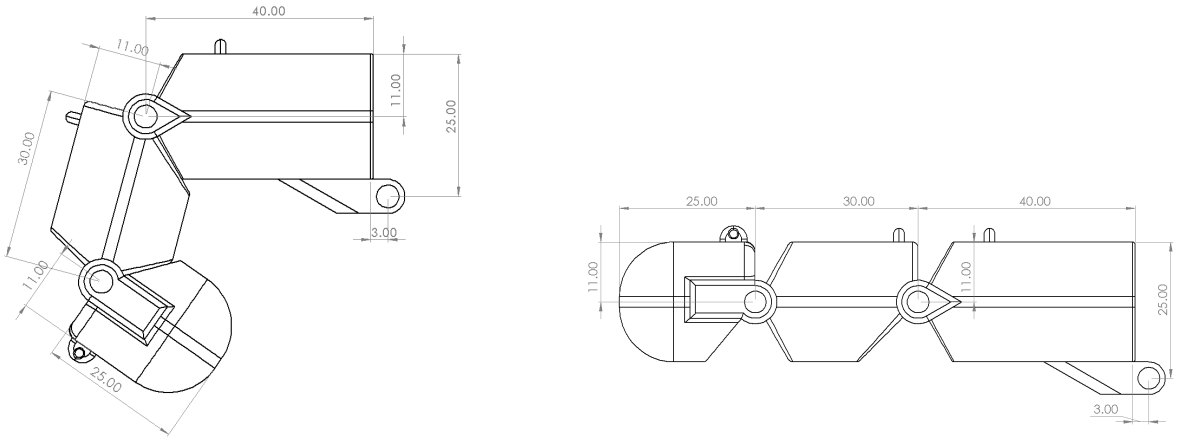

(a) mid-finger curved

(b) mid-finger extended

Figure 9: mid-finger exoskeleton design

By modelling the motion of each section of the finger as an arc, with the centre being the joint, we can deduced the extension of the rope through the equation:

$$\text{length of arc} = r\theta$$

Total displacement of the string overhead by calculation:

$$\begin{aligned}
\Delta L &= L_{DIP} + L_{PIP} + L_{MCP}, \quad \text{where} \\
L_{DIP} &= 11 \times \frac{45}{360} \times 2\pi \approx 8.64, \\
L_{PIP} &= 11 \times \frac{60}{360} \times 2\pi \approx 11.52, \\
L_{MCP} &= (25 - 11) \times \frac{85}{360} \times 2\pi \approx 20.77 \\
\Rightarrow \Delta L &\approx 8.64 + 11.52 + 20.77 = \boxed{40.93\text{mm}}
\end{aligned}$$

Wrist Movement

The two degrees of freedom in our wrist are flexion/extension and radial/ulnar deviation, with the two rotational centre almost coinciding, it becomes difficult to design the mechanical structure of the exoskeleton. Thus, we designed a mechanism that is functionally similar to a universal joint, see Figure 10. The palm is represented as an oval, and the linkage structure connecting the fingers to the palm allows the 2 DOF in the MCP joint.

For the robotic hand exoskeleton, there are a total of 22 links and 20 joints, giving rise to 22 DOFs in the hand exoskeleton.

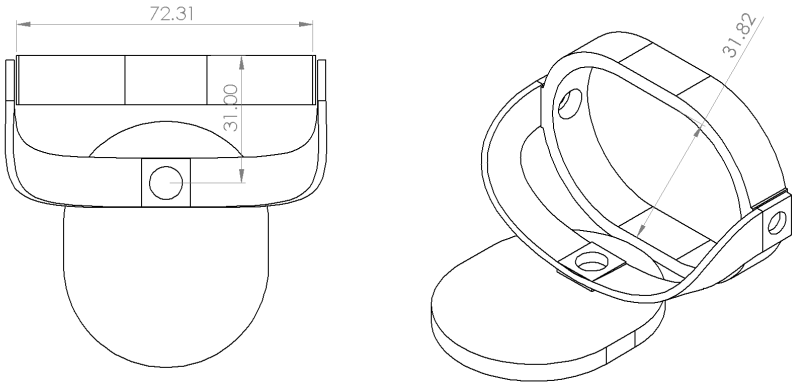

Figure 10: demostration of wrist

3.2 Wolf Claw Mechanism V I: Planetary Gear with Mechanism Analysis

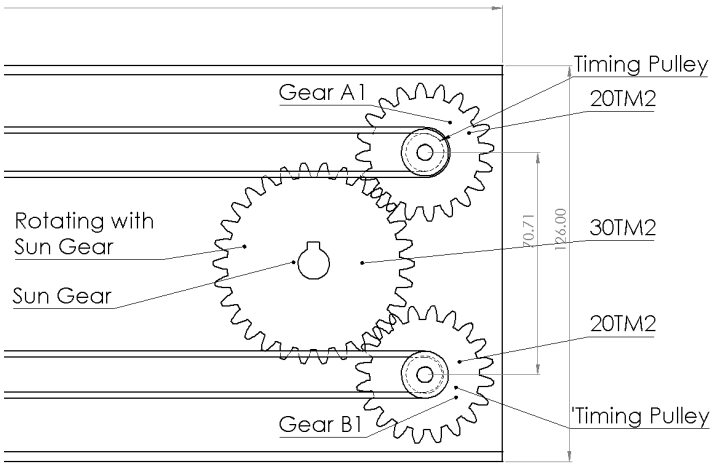

Figure 11: gear A_1 and B_1

A schematic diagram of version one's planetary gear is shown in Figure 12. The planetary gear is a fixed carrier gear, with the carrier (illustrated in dark blue) fixed to the upper

inner surface of the housing using three screws. The sun gear is extended downwards to mesh with two identical spur gears A_1 and B_1, see figure 11, secured to the base of the housing using screws, forming a simple secondary gear train. To convert this rotary motion into linear motion, two identical gears A_2 and B_2, timing pulleys, are screwed to the bottom of the box, parallel to A_1 and B_1 (the screws are not tight, the timing pulleys and gears A_1 and B_1 can still rotate about its centre of rotation, the screw). The end of gears A_1 and B_1 are glued into timing pulleys, timing belts connect A_1–A_2 and B_1–B_2, forming two pulley and belt systems, enabling low-noise transmission without slippage, see Figure 4.

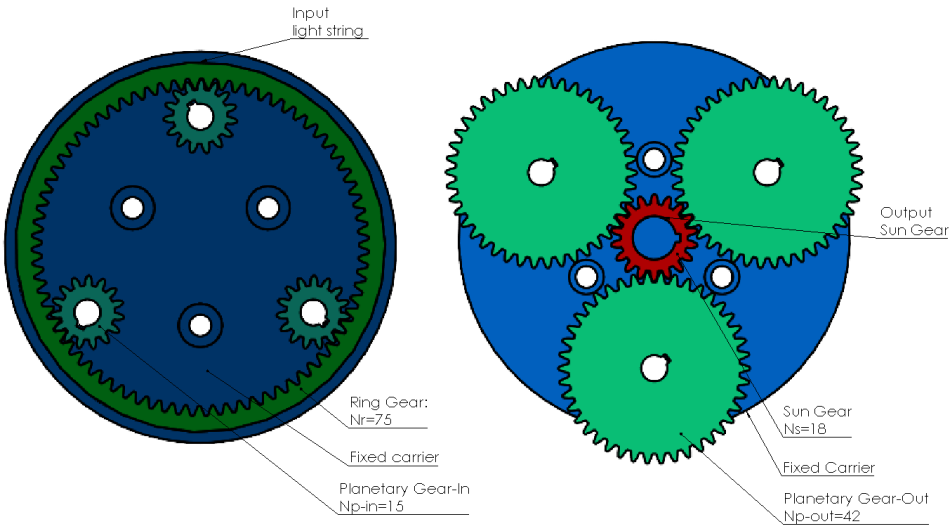

Figure 12: Kinematic scheme of the planetary gear mechanism

The design parameters of the planetary gear system are summarised as followed: The sun gear has 18 teeth, the inner and outer sides of the compound planet gear have 42 and 15 teeth respectively, and the ring gear has 75 teeth, satisfying the concentric condition

$$N_r = N_s + N_{\text{p-in}} + N_{\text{p-out}} = 75$$

Each of the two secondary gears A_1 and B_1 has 36 teeth, and three identical compound planet gears are evenly distributed at $120\,\text{deg}$ intervals to maintain torque balance and provide structural stability.

The assembly conditions are fulfilled by the following expression:

$$\frac{N_s N_{\text{p-out}} + N_r N_{\text{p-in}}}{3} = 1140 \in \mathbb{Z}$$

The side blades are fixed to the sides of the belt system using two screws near the end to prevent detachment. The three blades are connected with the two side blades providing a driving force to the centre blade, this centre blade is connected to a third pulley and belt system to increase stability when the blades slide simultaneously. Belt tensioning is required to maintain a fully horizontal motion for blades (see Figure 4).

For a fixed carried planetary gear, the kinematic relationship between the angular velocities of the ring and sun gears can be expressed using Willis equation:

$$\frac{\omega_r - \omega_c}{\omega_s - \omega_c} = -\frac{N_s}{N_r}, \text{ since } \omega_c = 0 \tag{1}$$

$$\Rightarrow \frac{\omega_r}{\omega_s} = -\frac{N_r}{N_s} \tag{2}$$

The transmission ratio of the compound planetary gear system is then given by:

$$i_{\text{planetary}} = 1 + \frac{N_r N_{\text{p-in}}}{N_s N_{\text{p-out}}} = 1 + \frac{75 \times 42}{18 \times 15} \approx 12.7 \tag{3}$$

After the planetary stage, the sun gear is connected with another gear (30 teeth) that directly drives the two identical spur gears A_1 and B_1 (36 teeth each). The secondary gear ratio is therefore:

$$i_{\text{secondary}} = \frac{Z_{A_1}}{N_s} = \frac{36}{30} = 1.2$$

In the belt transmission stage, the linear velocity of the belt is related to the angular velocity of the pulleys by:

$$\begin{cases} v_{\text{belt}} = r\,\omega_{\text{pulley}}, \\ x = r\,\theta_{\text{pulley}} \end{cases}$$

Since both pulleys have equal radii and the displacements of the left, centre, and right blades are identical:

$$x_L = x_C = x_R = r\theta$$

The overall transmission ratio of the complete mechanism can thus be expressed as:

$$N_{\text{total}} = N_{\text{planetary}} \times T_{\text{secondary}} \times i_{\text{belt}} = 12.67 \times 1.2 \times 1.0 = 15.2$$

Therefore, the total theoretical transmission ratio of the system is approximately $i_{\text{total}} = 15.2 : 1$, providing significant torque amplification and smooth synchronised blade extension. The general expression for the total transmission ratio can be written as:

$$i_{\text{total}} = \left(1 + \frac{N_r N_{p-\text{in}}}{N_s N_{p-\text{out}}}\right) \times \frac{Z_{A1}}{N_s} \times \frac{r_{A_2}}{r_{A_1}}$$

Figure 3 illustrates the relationship between the input ring gear angle, θ_r, and the output sun gear angle, θ_s, derived from equations (2) (3). The results demonstrate a linear inverse relationship between the two variables, with a gradient of -4.17, indicating opposite rotation directions of the input and output components and constant total transmission ratio throughout motion.

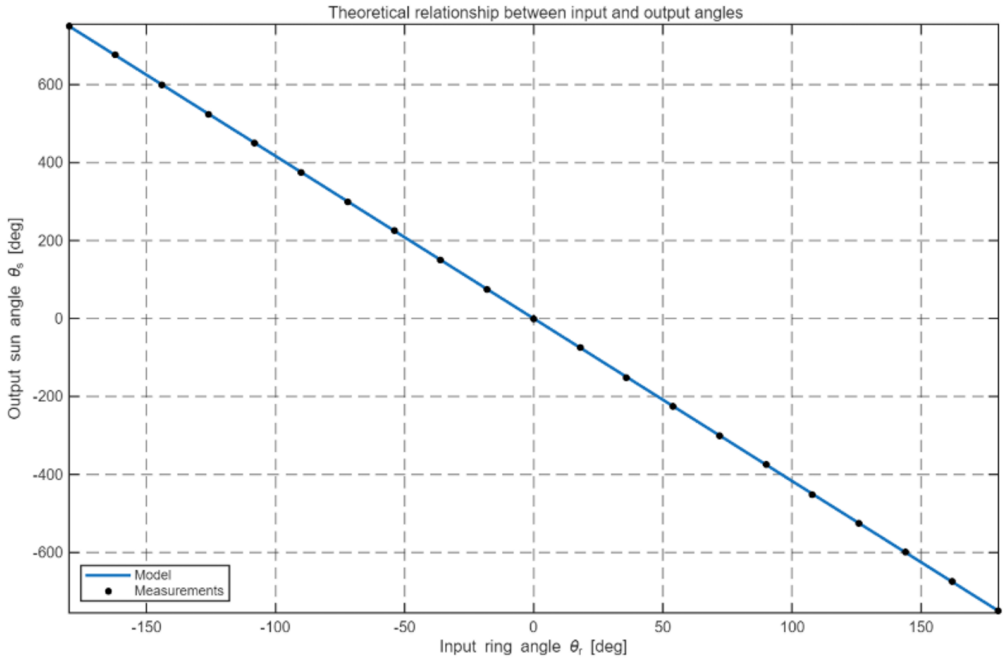

Figure 13: input and output angles relationship

The mathematical model satisfies all design requirements. The planetary gear stage provides a reduction ratio of approximately $12.7 : 1$, the secondary gear stage contributes an additional $1.2 : 1$ ratio, and the belt stage maintains a $1 : 1$ transmission. The total reduction ratio of $15.2 : 1$ enables high torque output while ensuring synchronized linear motion of the blades.

3.3 Wolf Claw Mechanism V II: Compound Gear Train with Mechanism Analysis

Version two replaces the compound planetary gear and the simple secondary gear train in version one with a compound gear train, simplifying assemble and improving torque transmission. The rope is connected to the drum of gear A, serving as the driving gear. Gears B and D form a compound pair as they are coaxial, transferring motion to the output gear, gear C. This framework achieves a higher torque output through two successive reduction stages, as shown in Figure 8a.

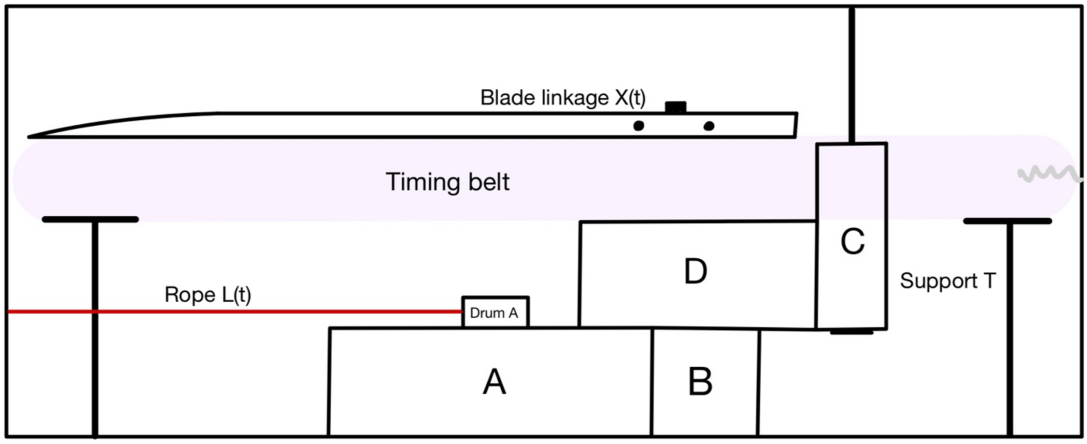

Figure 14: schematic of the compound gear-belt system showing motion transmission from the rope to the claw blades.

Let $S(t)$ be the normalized displacement of the rope, the fraction of total motion completed between $t = 0$ and $t = T$:

$$\begin{aligned} \ddot{S}(0) = 0, \quad \ddot{S}(T) = 0 \\ \dot{S}(0) = 0, \quad \dot{S}(T) = 0 \\ S(0) = 0, \quad S(T) = 1 \end{aligned}$$

These six boundary conditions ensure that the motion starts and ends smoothly (with zero velocity and acceleration at both ends), we use a 5th-degree polynomial to satisfy these six boundary conditions:

$$\begin{aligned} S(t) &= a_0 + a_1 t + a_2 t^2 + a_3 t^3 + a_4 t^4 + a_5 t^5 \\ \dot{S}(t) &= a_1 + 2a_2 t + 3a_3 t^2 + 4a_4 t^3 + 5a_5 t^4 \\ \ddot{S}(t) &= 2a_2 + 6a_3 t + 12a_4 t^2 + 20a_5 t^3 \end{aligned}$$

Substituting the boundary conditions into the above equations we have:

$$a_1 = 0, \quad a_2 = 0, \quad a_3 = 10\left(\frac{t}{T}\right)^3, \quad a_4 = -15\left(\frac{t}{T}\right)^4, \quad a_5 = 6\left(\frac{t}{T}\right)^5$$

The rope displacement, $L(t)$ follows a fifth-degree polynomial to ensure smooth motion:

$$L(t) = L_{\max} S(t),$$
$$S(t) = 10 \times (\frac{t}{T})^3 - 15 \times (\frac{t}{T})^4 + 6 \times (\frac{t}{T})^5$$

where $L_{\max}$ is the maximum rope displacement and T is the total motion time.

Since the rope is wound around a drum of radius r_{drum}, the angular displacement of gear A is:

$$\theta_A = \frac{L(t)}{r_{\text{drum}}} \quad (2)$$

For the gear train $(A \rightarrow B\&D \rightarrow C)$, the angular velocity relationships are:

$$\frac{\omega_A}{\omega_B} = -\frac{N_B}{N_A}, \qquad \omega_B = \omega_D, \qquad \frac{\omega_D}{\omega_C} = -\frac{N_C}{N_D}$$

Thus, the total transmission ratio between gears A and C is:

$$i_{\text{total}} = \frac{\omega_A}{\omega_C} = \frac{N_B}{N_A} \times \frac{N_C}{N_D}$$

and the angular displacement relationship is:

$$\theta_C = \theta_A \frac{N_A N_D}{N_B N_C}$$

Since the belt movement is directly proportional to the angular displacement of gear C, the linear displacement of the blade linkage can be expressed as:

$$x(t) = \frac{r_C N_A N_D}{r_{\text{drum}} N_B N_C} L(t)$$

Substituting $L(t) = L_{\max} S(t)$:

$$x(t) = \frac{r_C N_A N_D L_{\max}}{r_{\text{drum}} N_B N_C} S(t)$$

This equation defines the smooth linear motion of the blade linkage as a function of normalised time t. The total transmission ratio for the compound gear train is:

$$i_{\text{total}} = \frac{N_B}{N_A} \times \frac{N_C}{N_D}$$

Given $\frac{N_B}{N_A} = 3$ and $\frac{N_C}{N_D} = 4$, the total reduction ratio is $i_{total} = 12$.

This indicates that the blade linkage provides twelve times the input torque, with the overall design ensuring compact structure, high torque transmission efficiency, and smooth finger motion.

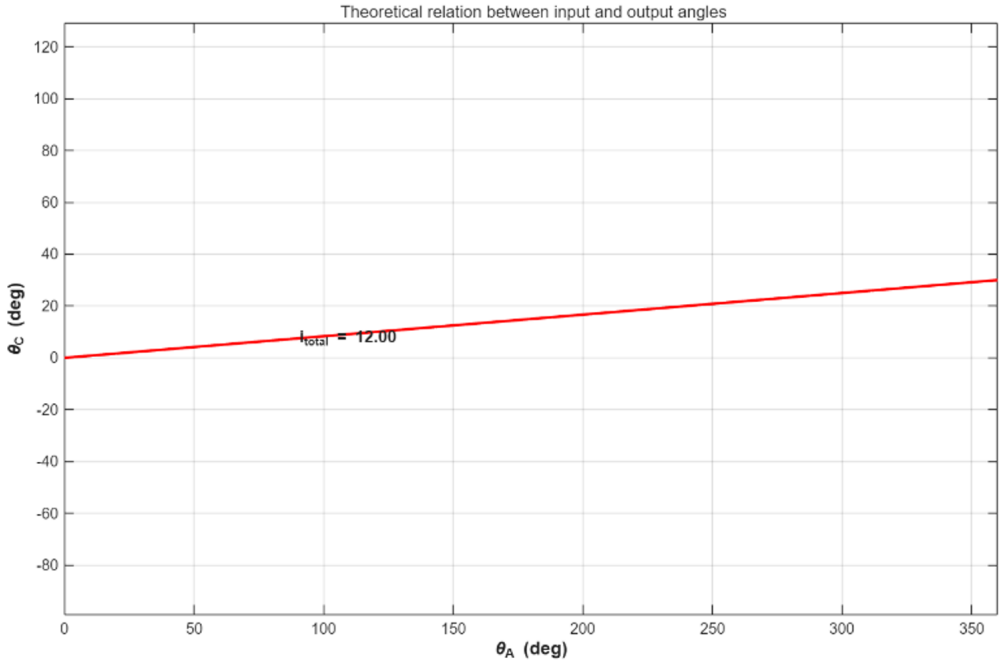

Figure 15: Theoretical relation between input and output angles

The Figure 15 illustrates the linear relationship between the input gear rotation, θ_A, and the output gear rotation, θ_C, in the compound gear train. With the gradient representing the overall transmission ratio $i_{\text{total}} = 12$.

4 Conclusion and Future Work

Our design proposes a lightweight, passive mechanism that relies on the user's intuitive actions. The DOFs of the exoskeleton hand closely matches the DOFs of a human hand, excluding the unnecessary rotations (which would lead to a lower efficiency). With the two wolf claw mechanisms involving rotary-to-rotary transmission and rotary to translational transmission.

Moving forward, experiments would be run to investigate what would be considered a "safe" distance, average reaction time and speed of waving your arm. We will then adjust the gear ratios for our first prototype accordingly and integrate damping for shock absorption into this apparatus, whilst minimising the size of the housing for the wolf

claw mechanism. During this process, we will be focussing on implementing the non-backdrivable feature throughout the whole mechanism as our first prototype only includes this in the spring plungers at the side blades. Though we could design the open timing belt such that it operates as a ratchet and connect a pawl to the side of the box using springs, the manufacturing of the ratchet would be troublesome as each section would have to be 3D printed individually, and the removal of these supports (from 3D printing individual sections) would be toilsome.

References

[1] Pilwon Heo, Gwang Min Gu, S. J. Lee, et al. Current hand exoskeleton technologies for rehabilitation and assistive engineering. *International Journal of Precision Engineering and Manufacturing*, 13:807–810, 2012.

[2] Office for National Statistics. Stalking: findings from the crime survey for england and wales (csew) year ending march 2025, 2025. Data extracted from Table 1 and Table 5.

[3] Jacob Rosen. *Wearable robotics: Systems and applications*. Academic Press, 2019. chapter 8.

[4] Jacob Rosen. *Wearable robotics: Systems and applications*. Academic Press, 2019. chapter 9.

[5] UK Gov. Criminal justice and immigration act 2008. `https://www.legislation.gov.uk/ukpga/2008/4/contents`, 2008. Accessed: 2023-10-01.